

Mapping the Effects of Hurricane Michael and Biological Drivers of Change on Seagrass in St.  
Joseph Bay, Florida

by

Allison Senne

A thesis submitted in partial fulfillment  
of the requirements of the  
University Honors Program  
University of South Florida, St. Petersburg

May 6, 2020

Thesis Director: Paul R. Carlson Jr., Ph.D.  
Instructor, College of Arts and Sciences

University Honors Program  
University of South Florida  
St. Petersburg, Florida

CERTIFICATE OF APPROVAL

---

Honors Thesis

---

This is to certify that the Honors Thesis of

Allison Senne

has been approved by the Examining Committee

on May 6, 2020

as satisfying the thesis requirement

of the University Honors Program

Examining Committee:

---

Thesis Director: Paul R. Carlson Jr., Ph.D.

Instructor, College of Arts and Sciences

---

Thesis Committee Member: James Ivey, Ph.D.

Instructor, College of Arts and Sciences

## **ABSTRACT**

Hurricane Michael in October of 2018 was ranked third in intensity out of all the hurricanes that have ever been recorded to strike the United States. It struck in the Panhandle of Florida as a Category 5 on the Saffir-Simpson scale, and cost close to 30 billion dollars in damage. Damages to the status, health and distribution of seagrass beds, which are a key component of coastal ecosystems globally, have yet to be assessed. For this study, seagrass was digitized and mapped from aerial imagery taken in 2019 of St. Joseph Bay. The goal of this study was to assess the changes in seagrass cover that took place between 2017 and 2019. These changes are a result of Hurricane Michael as well as other drivers of change including but not limited to factors such as water quality, benthic morphology, and possibly other biotic factors. When the mapping was completed, this was compared with seagrass cover maps made of St. Joseph Bay in previous years (1959, 1980, 1992, 2003, 2010, 2015, and 2017). The results of this study suggest that 40.38% of existing seagrass meadows in St. Joseph Bay from 2017 to 2019 experienced a cover decline, 2.49% experienced a cover gain, while 57.13% of seagrass experienced no cover change. It is necessary to monitor them, as they are an invaluable indicator species for both natural and human environments.

## **ACKNOWLEDGEMENTS**

I would like to express my sincere gratitude to Dr. Paul Carlson and Dr. Laura Yarbrow, Research Scientists in the Seagrass Habitat Laboratory at the Florida Fish and Wildlife Conservation Commission for guiding me in this venture and providing all the necessary facilities for the research. My internship with them at the Fish and Wildlife Research Institute has been an invaluable resource for experiential knowledge and hands-on learning.

I place on record, my sincere appreciation to Dr. James Ivey, Instructor of Environmental Science Policy at the University of South Florida St. Petersburg, for his encouragement and guidance.

I am also grateful to Dr. Thomas Smith, Honors Program Director at the University of South Florida St. Petersburg for his unwavering support and guidance during my entire educational journey at the University of South Florida St. Petersburg.

I take this opportunity to express my thanks to Elizabeth Johnsey for her expertise and availability to answer my questions as well as help me navigate through the complicated technology applications.

I also place on record, my sense of gratitude to one and all, who directly or indirectly, have lent their hand in this year-long senior thesis project.

## CONTENTS

### Introduction

Seagrasses and Study Area.....	1
Hurricane Michael.....	4
Sea Urchins.....	6

### Methods

GIS Procedure.....	8
GIS Data Layers.....	9
Creating the 2019 Seagrass Cover Map.....	9
Calculating Percent Cover Change.....	14

### Results and Discussion

Maps.....	17
Calculated Areas of Total Seagrass Cover Loss, Gain, and No Change.....	21
Calculated Percentage Distribution of Seagrass Cover Loss, Gain, and No Change....	22

Conclusion.....	25
-----------------	----

Works Cited.....	26
------------------	----

Appendices.....	29
-----------------	----

## INTRODUCTION

### Seagrasses and Study Area

In the state of Florida, about 14 million people live along the famous peninsular coastline, which is around 67% of the state's population (NOAA, 2019). Many of these people are unaware of just how much of their coastal existence relies on just one order of plants; Alismatales, or seagrass. Seagrasses are marine monocotyledons, which means that they are a flowering plant. This is because they “evolved from a single lineage of monocotyledonous flowering plants between 70 million and 100 million years ago” (qtd. in Orth et al, 2006). Unlike colonizing marine plants, seagrasses have an extremely low species diversity totaling in about 60 individual species, which is relatively low considering that there are about 250,000 species of terrestrial monocotyledons (Orth et al, 2006). Despite their low species diversity and distinct physiological characteristics, seagrasses have successfully colonized every ocean, save for the poles. (Orth et al, 2006).

These plants are also heavily influenced by light, requiring some of the highest light levels of any plant group, which results in a high sensitivity to environmental change as well as phenological sensitivity (Orth et al, 2006). Subsequently, seagrass meadows in Florida waters become robust and abundant in the summer months due to having more than sufficient amounts of sunlight and heat. During this time in St. Joseph Bay, Florida, seagrass biomass and density peaks near 150 g ash free dry weight/m<sup>2</sup> and approximately 3000 leaves/m<sup>2</sup> during summer months (Valentine and Heck, 1993). The converse is true for the winter months, as their productivity declines with less sunlight and lower tides that can expose them to the air.

Their importance is derived from the priceless natural services that these plants provide for both the anthropocentric world as well as entire ecosystems. To start, Seagrasses help to maintain the physical shape of the coastline as they anchor sediments with their root systems and absorb energy from wave action that would otherwise erode the coast as well as change the littoral morphology quickly and drastically without their presence and abundance (Larkum et al, 2011). Seagrasses also support marine life by acting directly as a food source, or as a nursery and habitat for a diverse array of species. Commercial as well as recreational inshore fishing in Florida particularly relies on many of these same species such as tarpon, snapper, and grouper (Matz, 2015). Tourism centered around species which are considered megafauna such as manatees and sea turtles, is equally important with regards to the economy of Florida (FWC). Recently, it has even been observed that when in good health, seagrasses can disinfect surrounding water of bacteria that is harmful to both fish and humans by producing a natural biocide (Lamb et al, 2017). As a result of these ecosystem services as well as many more unmentioned, these grasses are worth over \$19,000 per hectare, according to Smithsonian Ocean, making them the third most valuable ecosystem in the world.

Far from seaweed, these grasses are intrinsically priceless, as they promote and directly support much of the biodiversity that are characteristic of coastal and marine ecosystems. Seagrasses are simultaneously nicknamed “ecosystem engineers” because they establish the base of many marine food webs. Seagrasses are also often referred to as “coastal canaries” since they are exposed to multiple stressors, therefore making them vulnerable. If they begin to fail, then the rest of the surrounding food web will also follow suit. Seagrasses are representatives of the health and status of both their own ecosystem and those surrounding them, including human environments and economies.

Since seagrasses can be considered the metaphorical backbone of their seascape, their great importance causes them to constantly experience stressors in the form of physical and biological disturbances. Not only that, but disturbances to seagrasses have a greater effect on coastal ecosystems. These disturbances include but are not limited to herbivores, competing producers, tides and air exposure, hurricanes, storm surge, water quality, and turbidity (FWC). Perhaps the greatest threat to seagrasses globally are humans and our various exploits. This is because the world's population has historically resided, developed, and polluted coastally as well as around areas such as bays and estuaries, which happen to be where seagrasses are most abundant and biogeographically important to the environment (Griffiths et al, 2020).

Shipping and industrial ports are responsible for much of the direct anthropogenic seagrass loss around the world. This same genre of human endeavor also is typically economically successful, but there would be no coastal economy or community for humans if marine ecosystems collapse. Not only do they directly and consistently pollute waters where seagrasses thrive and introduce invasive species, but they also invite increased development which requires increased dredging and expansion of shipping routes for boats that are getting bigger to accommodate globalized commerce (Florida Museum, 2018). Dredging of bays and estuaries results in the direct destruction of seagrass meadows through their physical removal and burying. This process stirs up the sea bottom, increasing the turbidity of the water which can block sunlight from reaching the seagrass. As previously discussed, this increased turbidity and light attenuation has a negative effect on seagrass' rates of productivity and photosynthesis. Whether or not seagrasses can survive this varies greatly between seagrass species and depends primarily on the biochemical structure, shape, and size of the individual blades (Erftemeijer and Lewis, 2006).



While all of these are factors that will always influence the status, health, and productivity of seagrass meadows, this study focuses particularly on the seagrass loss due to Hurricane Michael in 2018 as well as sea urchin grazing. To quantify and analyze the seagrass loss caused by these processes, seagrass meadows were mapped in St. Joseph Bay of Florida's Big Bend region in the northern Gulf of Mexico. The bay is approximately 24 kilometers long and 9.7 kilometers wide, with a distinctive peninsula making up the whole of St. Joseph Peninsula State Park. The waters of the bay contain St. Joseph Bay State Buffer Preserve and the St. Joseph Bay Aquatic Preserve in its internal waters. St. Joseph Bay in particular "is dominated by large monospecific stands of *Thalassia testudinum* interspersed with smaller patches of *Halodule wrightii*, unvegetated sand flats and small amounts of *Syringodium filiforme*" (Valentine and Heck, 1993). Data collected by the Florida Fish and Wildlife Commission from 2008, 2009, 2011, and 2014 indicated that the occurrence of seagrass species was stable but that the density of seagrass beds was variable and thinning (Yarbro and Carlson, 2016). Increased and extensive propeller scarring is also evident in St. Joseph Bay, as it is a popular recreational bay scallop (*Argopecten irradians*) fishery.

## **Hurricane Michael**

In the United States, Florida is famously the recipient of many Atlantic hurricanes that make landfall. Because historical records of hurricanes in the United States only date back to around 1870, there is not enough data to confidently and accurately claim that hurricanes are increasing in either power, frequency, or duration (Knutson et al 2020). However, since around 2000, there has been an alarmingly high number of hurricanes and tropical storm systems with record breaking intensities and destruction. This is partly due to the increased development and infrastructure where these storms have made landfall, meaning that there is now more to be

destroyed and lost than in the past. Two commonly registered disturbances by hurricanes in shallow seagrass beds are burial and sediment removal.

Hurricane Michael in October of 2018 is ranked as third most intense out of all the recorded hurricanes to have struck the continental United States. It traveled north up the Gulf of Mexico and hit the Big Bend region of Florida's panhandle, including St. Joseph Bay, causing 30 billion dollars in catastrophic damage to multiple coastal towns. In St. Joseph Bay the storm surge created an inlet in the peninsula that had not previously existed, slicing the St. Joseph Peninsula State Park in half along with the road that spanned it. While property and infrastructure damages have been scrutinized and calculated, damages that this storm caused to the environment and impairment of natural ecosystem services have yet to be fully assessed.

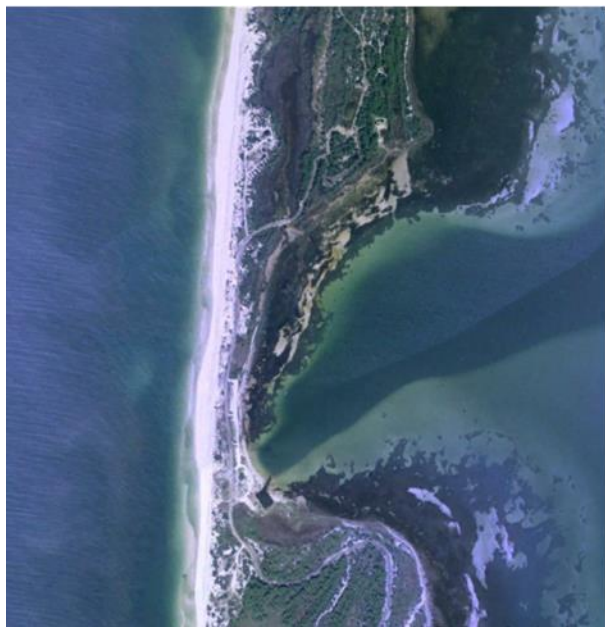


**Figure 1:** Satellite imagery from Google Earth of St. Joseph Peninsula State Park in 11/2007

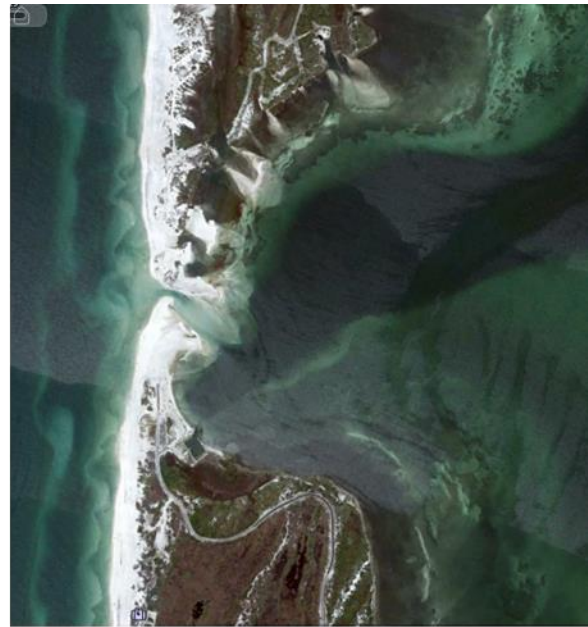


**Figure 2:** Satellite imagery from Google Earth of St. Joseph Peninsula State Park on 4/27/2019

## Sea Urchins

Sea urchins are extremely effective, important, herbivorous members of the phylum Echinodermata, meaning that they are marine animals with radial symmetry, usually with five points or more in adults ("*Asterias forbesi*"). They also possess many tube feet, a water vascular system, and an endoskeleton made of primarily calcium carbonate, much like other shelled organisms (Wray, 1999).

Sea urchins are commonly known for their insatiable appetite for kelp forests, but in Florida since the 1970s, it has been observed and documented that sea urchins have the capacity to overgraze and defoliate large areas and densities of seagrass along the west coast (Valentine and Heck, 1993). This occurs when the urchin population overwhelms a meadow of seagrass. Urchins reproduce sexually, usually externally, but also can regenerate and reproduce asexually via fragmentation. *L. variegatus*, the sea urchin known as the green sea urchin or the variegated sea urchin, “previously observed defoliating large expanses of seagrass in the northern Gulf of Mexico is commonly found within vegetated areas of St. Joseph Bay with population densities as high as 140 individuals/m<sup>2</sup>” (Valentine and Heck, 1993). These events are known as overgrazing and are classified as such when they have large size as well as impairment of ecosystem services. The scientific community lacks an in depth understanding of the drivers and mechanisms by which these overgrazing events occur, but there are several hypothesized factors that are plausible, all of which are related to a heavy human presence and disturbance. These include eutrophication due to runoff from various point and non-point sources, overfishing of the sea urchin’s natural predators, and rising water temperatures. The sea urchin’s natural predators include fish, shorebirds, gulls, Echinoderms like sea stars, and cassis Gastropods, known as helmet snails (Sweat 2012). These potential drivers often interact and occur together, especially

in areas with high anthropogenic pressure, suggesting that multiple disturbances are at work. By inadvertently reducing predation, urchin recruitment increases and reduces the resistance of seagrasses, which could potentially pave the way for overgrazing events. (Eklöf et al, 2008).

A study from 2019 concerning sea urchin populations in St. Joseph Bay after Hurricane Michael supported the idea that sea urchins within the seagrass communities in the northern Gulf of Mexico are resilient to hurricanes (Challener et al., 2019).

## METHODS

### GIS Procedure

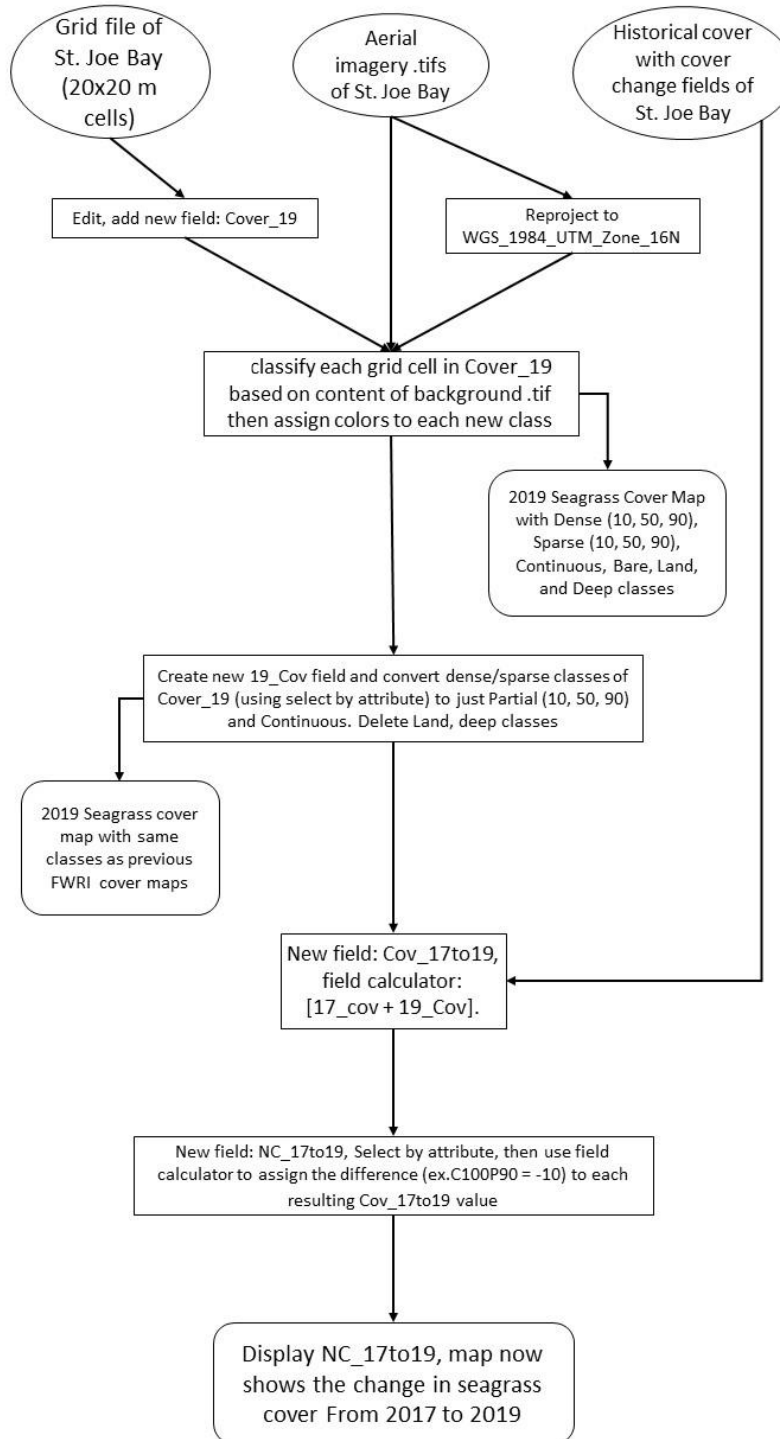


**Figure 3:** Flowchart of GIS Procedure used for mapping and data collection. Circles represent input data layers, rectangles represent processing, while rounded rectangles represent produced map layers.

## **GIS Data Layers**

Three main layer groups were manipulated within ESRI's ArcMap 10.3.1 for this analysis. Since the imagery used in this study had a high resolution of 10215x10215 pixels, it was added to the ArcMap with one layer per .tif tile, with over 40 tiles. With the tiles re-projected and properties changed so that their background was opaque, these tiles do not overlap each other and complete the full extent of the bay so they function as the first layer group. The second layer group consists of six different 20x20 meter grid shapefiles with both cover and cover change attributes for each cover study completed by the Fish and Wildlife Research Institute (FWRI). These will be merged later with the Cover 19 grid. The third, topmost layer is a 20x20 meter grid shapefile with an empty Cover19 field.

The properties of this grid are changed so there is no color fill to the cells, and the aerial imagery can be clearly seen beneath. This layer is to be edited the most and will contain the completed cover and cover change analysis maps. The first and third layers remain active during data collection while the second and third layer remain active during data processing and analysis.

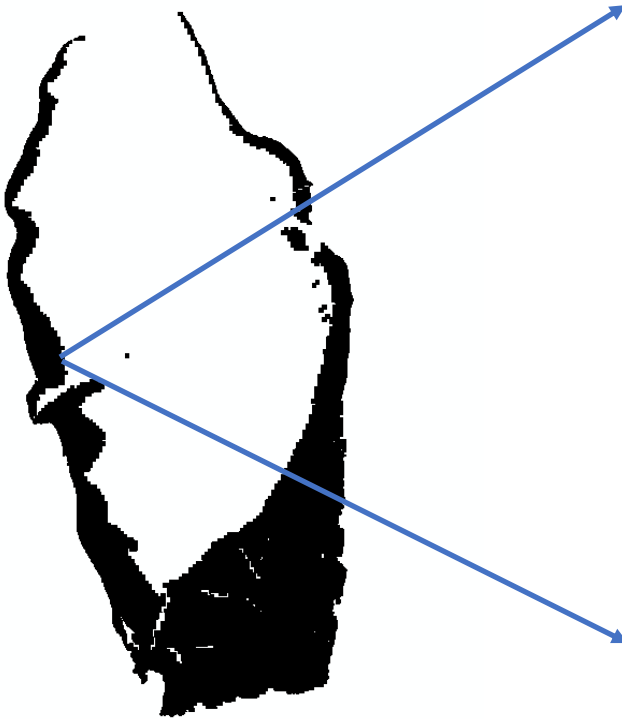
## **Creating the 2019 Seagrass Cover Map**

Currently there is not an accurate automated method that can detect the presence of seagrass and then classify it as such, instead only user photointerpretation and semi-automated methods. Present day LiDAR and remote sensing abilities are restricted in the case of seagrass mapping due to how the properties of light function underwater with suspended particles as well as turbidity. The issue lies with the beam of light that terrestrial LiDAR sensors use to create an image, usually near infrared with wavelengths between 1000 – 1500  $\mu\text{m}$ , most commonly used with a solid-state laser that produces an infrared frequency of 1064 nm. These frequencies are

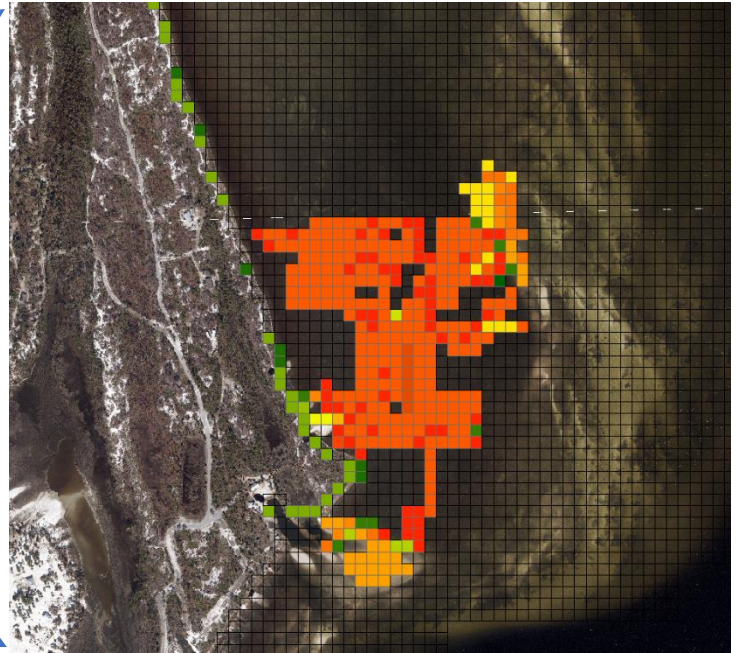
too large to penetrate the surface of the water and are often absorbed at the water surface. Most topo-bathymetric aerial LiDAR systems utilize the blue-green wavelength, still with a solid-state laser, but has a frequency of double that of the terrestrial, 532 nm. This level of output can penetrate the surface of a body of water, “however signal strength attenuates exponentially through the water column” in accordance with Beer’s law (Nayegandhi, 2007).

This study used aerial imagery taken of St. Joseph Bay Florida and generated by Kucera International Inc, for the Florida Fish and Wildlife Commission’s Fish and Wildlife Research Institute in 2019, several months after Hurricane Michael. The imagery was taken under optimal conditions of cloud cover, water quality, sun light, and sun angle. This was then loaded as .tif files into ESRI’s ArcMap program to create a map. Since these files are very large with a high resolution, the scale of the data frame from which the classifications were made was set to 1:1250 as a controlled variable.

Next, all the aforementioned tiles needed their projection changed to Universal Transverse Mercator, or UTM. This was done because afterwards, a grid downloaded from the Fish and Wildlife Commission in the UTM projection was laid over the imagery tiles. The grid consists of approximately 109395 grid cells each with an area of 400 m<sup>2</sup>, and follows the interior perimeter of St. Joseph Bay, including the littoral zone where seagrass meadows are located and distributed. The grid layer’s attributes were then edited by first creating a feature for seagrass coverage in 2019. The grid as well as the classification process are depicted in figures 4 and 5.



**Figure 4:** Full extent of the St. Joe Bay grid



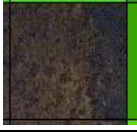









**Figure 5:** Zoomed grid portion depicting example of classified squares overlaid onto high resolution aerial imagery

Once the new Cover 19 feature class was created in the grid's attribute table, each of the grid cells were classified based off user photointerpretation of their seagrass content and cover, objectively assigning one classification label per grid cell. Figure 2.4 contains the key that was used for this classification.

Techniques to achieve this quickly and efficiently are made possible with the tools and features provided by ArcMap, as it is much too time consuming and therefore inefficient to classify one square at a time. These tools and features include but are not limited to highlighting, de-selecting highlighting, and the field/classification calculator within the attribute table.



Class	Code	Example
Dense Continuous	DC100	
Dense Patchy 90%-50%	DP90	
Dense Patchy 50%-10%	DP50	
Dense Patchy 10%-1%	DP10	
Sparse Continuous	SC100	
Sparse Patchy 90%-50%	SP90	
Sparse Patchy 50%-10%	SP50	
Sparse Patchy 10%-1%	SP10	
Bare	BARE	
Land (above sea level)	LAND	

**Figure 6:** Photointerpretation key with examples from imagery

It is relatively easy to observe the boundary between shallow and deep water with this imagery, because the camera cannot detect the hues at the bottom of the bay. While there actually might be seagrass present, the water is too deep and therefore dark for the sun's light to reflect and reach back to the aerial camera, so it is thusly absorbed by the water, appearing dark in the imagery. For the tiles that do not contain any land features, the darkest and deepest areas produced a visible pixelated feedback on the surface that appears to be capillary waves. However, this is different from wave action or fetch, as they further obscure the view and feedback of the sea bottom.

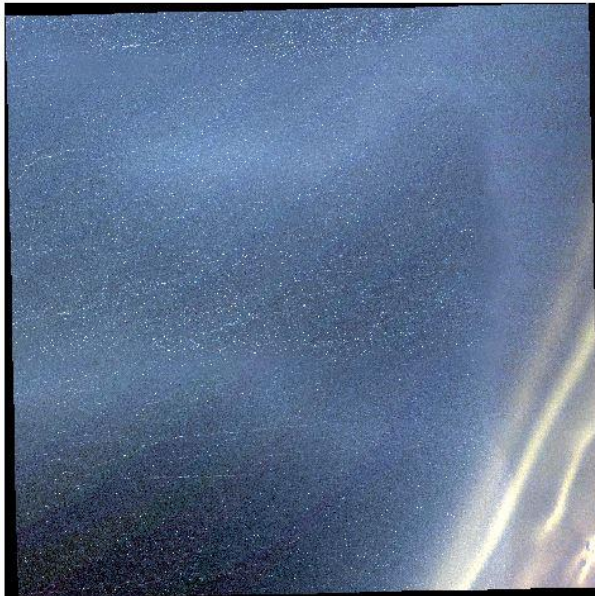


**Figure 7** Example of imagery tile with no land and pixelated feedback



**Figure 8** Example of imagery tile with land and wave fetch/chop

After completely classifying the attributes of the Cover19 field and exporting the grid shapefile to permanently save it as a layer, an additional field was added to the grid's table. The purpose of this field is to re-classify the 'Cover19' field, so it has the same classifications as the historical seagrass cover maps in St. Joseph Bay. This field was named 19\_Cover, to match the

format of the previous cover data, as well as stand apart from the preliminary Cover19 field.

These conversions were made by using ‘Select by Attribute’ tool for the Cover19 field and ‘Field Calculator’ for calculating the following values within the 19\_Cover field.

<b>Cover19</b>	<b>19_Cover</b>
LAND	LAND
BARE	BARE
DC100 , SC100	C100
DP90 , SP90	P90
DP50 , SP50	P50
DP10 , SP10	P10
DEEP	DEEP
No Imagery	No Imagery

**Figure 9** Conversion key from dense/sparse field to continuous/patchy field

After every square in every tile is re-classified, the count, percent of total cover, and area of each class of seagrass cover can then be calculated within Excel for any study year. These Results are shown in Appendices 1-3.

### **Calculating Percent Cover Change**

As part of the coordinated effort and partnership between National Oceanic and Atmospheric Administration (NOAA) and the Fish and Wildlife Research Institute (FWRI), seagrass has been mapped in the aforementioned method for the years: 1959, 1980, 1992, 2003, 2010, 2015, 2017, and now 2019. By comparing the historical cover data, seagrass cover and health can be analyzed temporally. This will be done by first spatially joining all the previous seven study’s shapefiles into one, with an attribute table that contains all the fields that were created during this process in addition to the historical cover data.

After creating and filling out the 19\_Cover field to match the historical cover data fields, 7 fields labelled ‘Cov\_YEARtoYEAR’ were added for each study period (example:

Cov\_17to19). The field calculator was used to fill each attribute with the value of [PreviousYear\_Cover + FollowingYear\_Cover] representing a change of their standardized classification of cover between study periods (example: 17\_Cover + 19\_Cover). There are 25 resulting classifications or values of this calculation, which correspond to the 25 possible combinations of cover change codes and represent the approximate total cover for every grid cell in the shapefile for two consecutive cover studies. (example: BAREBARE, or DP90DC100).

Next, another new field was added and labelled 'NC\_YEARtoYEAR' where 'NC' stands for numerical change in cover (example: NC\_17to19). The corresponding attribute field calculation was done by first selecting the attributes individually for each of the seven 'Cov\_YEARtoYEAR' fields where 'Cov\_YEARtoYEAR' = 'Result of [PreviousYear\_Cover + FollowingYear\_Cover]'. While the selection as well as 'view selection only' was still active, the difference of the integer within each of the 25 cover changes was calculated for each field's attributes. In other words, the resulting output in the 'NC\_YEARtoYEAR' field calculation is a 0, ±10, ±50, ±90, or ±100 integer from all the 'Cov\_YEARtoYEAR' values. This represents the percent cover change per grid cell that happened between each seagrass cover mapping and study. Figure 10 contains a chart that depicts this calculated relationship.

<b>Cov_YEARtoYEAR</b>	<b>NC_YEARtoYEAR</b>
C100C100	0
C100P90	-10
C100P50	-50
C100P10	-90
C100BARE	-100
P90C100	+10
P90P90	0
P90P50	-40
P90P10	-80
P90BARE	-90
P50C100	+50
P50P90	+40
P50P50	0
P50P10	-40
P50BARE	-50
P10C100	+90
P10P90	+80
P10P50	+40
P10P10	0
P10BARE	-10
BAREC100	+100
BAREP90	+90
BAREP50	+50
BAREP10	+10
BAREBARE	0

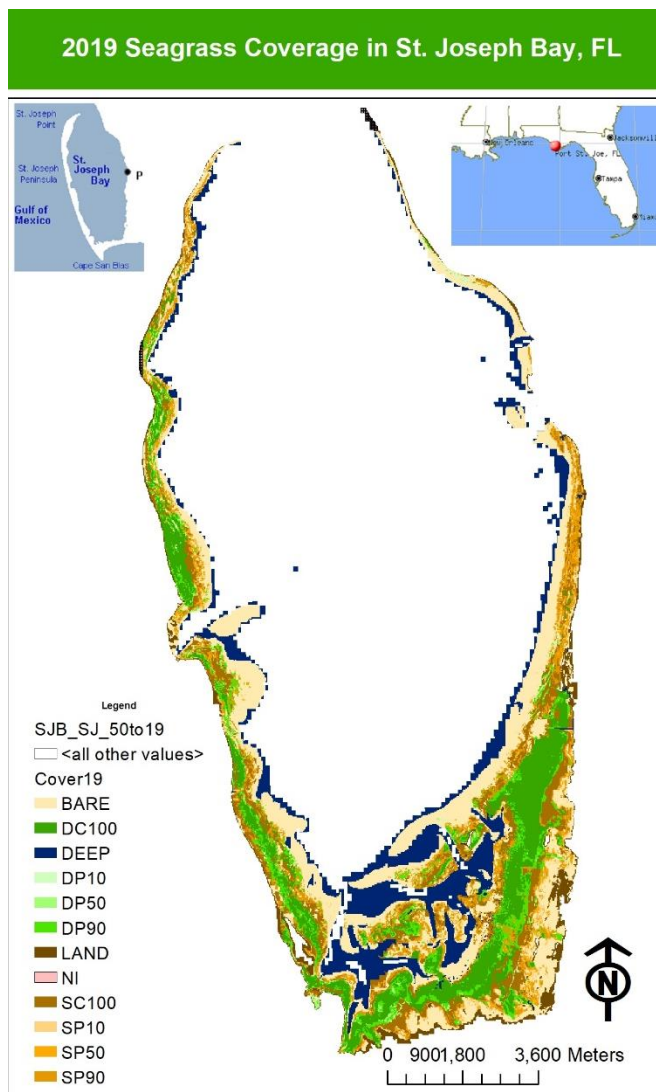
**Figure 10:** Conversion key for all possible combinations of percentage cover change with corresponding percent change value

Now, each NC\_YEARtoYEAR category can be displayed to show a map of percent cover change for each of the seven studies. Since this map shows the varying degrees of change for each grid cell, the color ramp chosen for each value of the NC\_YEARtoYEAR is on a spectrum from green to red, with the more positive values being green and the more negative values being red. The color for the 0 value was modified to a beige rather than the given yellow, so it would not distract from the areas of change.

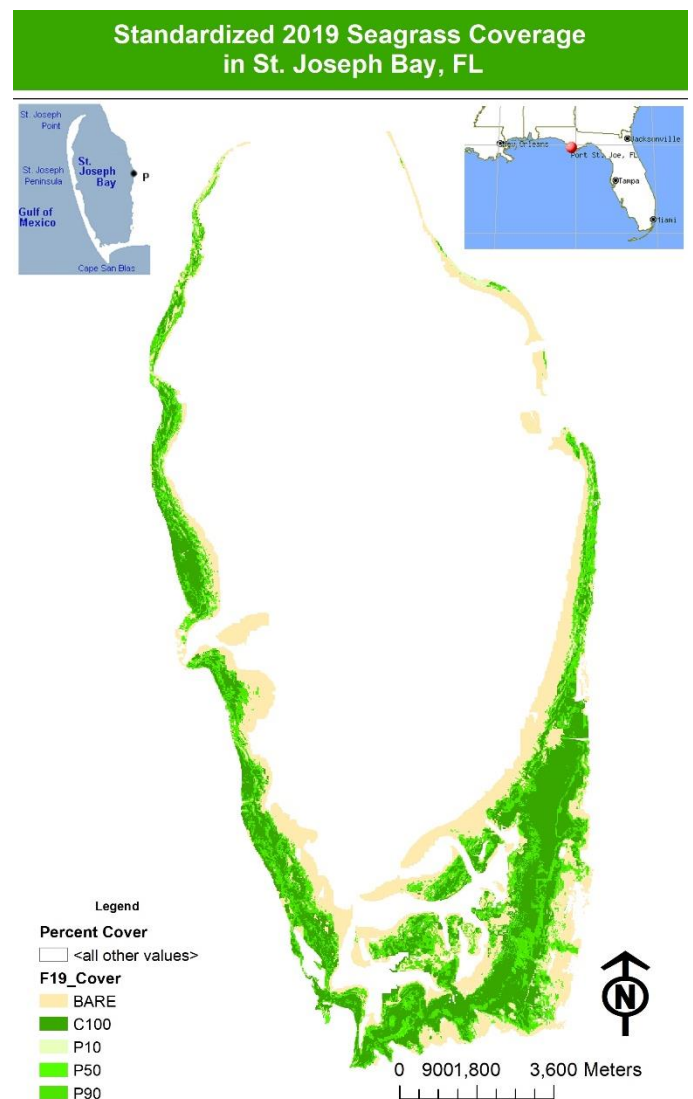
Finally, the frequency, area of cover, and subsequent percent of total cover for each class/value of cover change (0,  $\pm 10$ ,  $\pm 50$ ,  $\pm 90$ , or  $\pm 100$ ) can then be calculated within Excel for any study year. This was done for the six previous studies in addition to the 2019 study and graphed to aid with data interpretation. The frequency of grid cells that experienced any percent

of cover change was determined using the ‘Select by Attribute’ feature for each ‘NC\_YEARtoYEAR’ field, then each frequency was multiplied by the area of one grid cell (400 m<sup>2</sup>) to calculate the total area of seagrass that experienced any of the possible percent changes per grid cell. These calculations were then divided by the total area of the grid that contained bare sand or seagrass (109395 grid cells = 43758000 m<sup>2</sup>), which excludes classifications of land, deep water, and missing imagery to find the percent of the total study area that experienced each possible percent change.

## RESULTS AND DISCUSSION



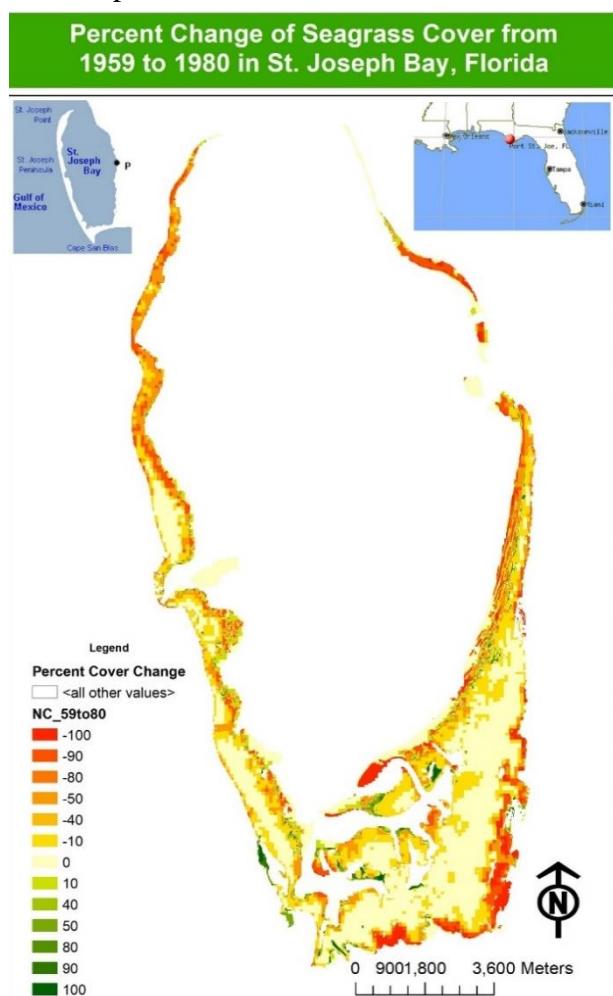
**Figure 11:** 2019 cover map of dense/sparse as well as continuous/patchy classes



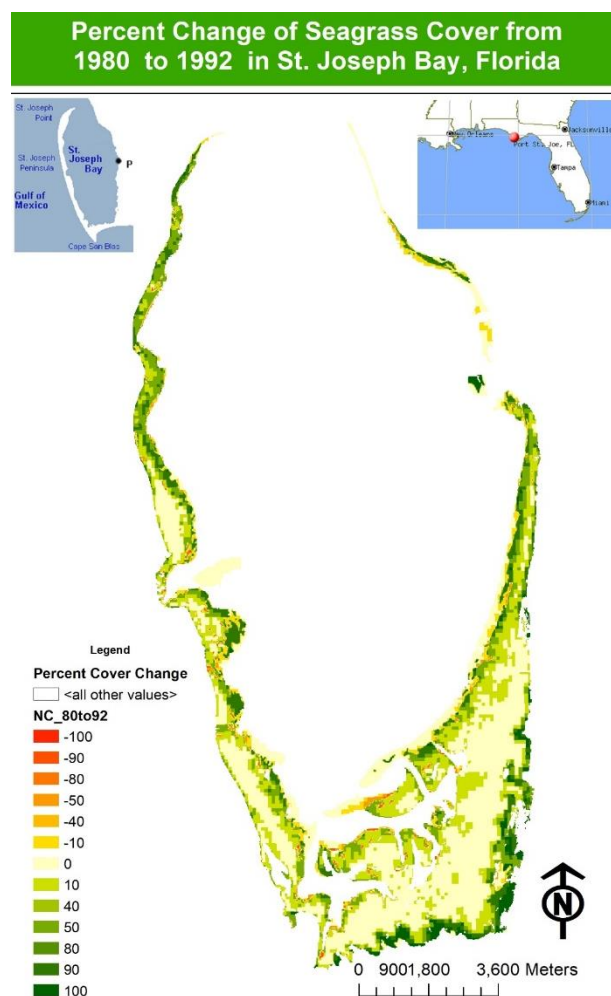
**Figure 12:** 2019 cover map of only dense/sparse classes to match previous cover maps



The preliminary classification of the Cover19 grid cells according to the provided and re-projected .tif format imagery tiles resulted in the map within figure 11. The scale is set at 1:94,708 in order to display the entire extent of the bay. Much of the shallow southern interior of the bay was too deep to classify between bare and seagrass, making the classification of dense or sparse also impossible, hence the need for a ‘DEEP’ classification. This could have been due to interpreter error, poor water quality, or storm surge from Hurricane Michael affecting the bathymetry of the bay. Figure 12 displays the cover data from 2019 with the same classifications as the historical FWRI cover data. Within this map there are no dense or sparse categories of classification, which correspond to the letter D or S in the legend. Additionally, the grid cells with ‘DEEP’, ‘LAND’, and ‘NI’ classifications were deleted as the historical data does not include these classes, decreasing the total area of the grid. The chronological results are seen in the maps below.

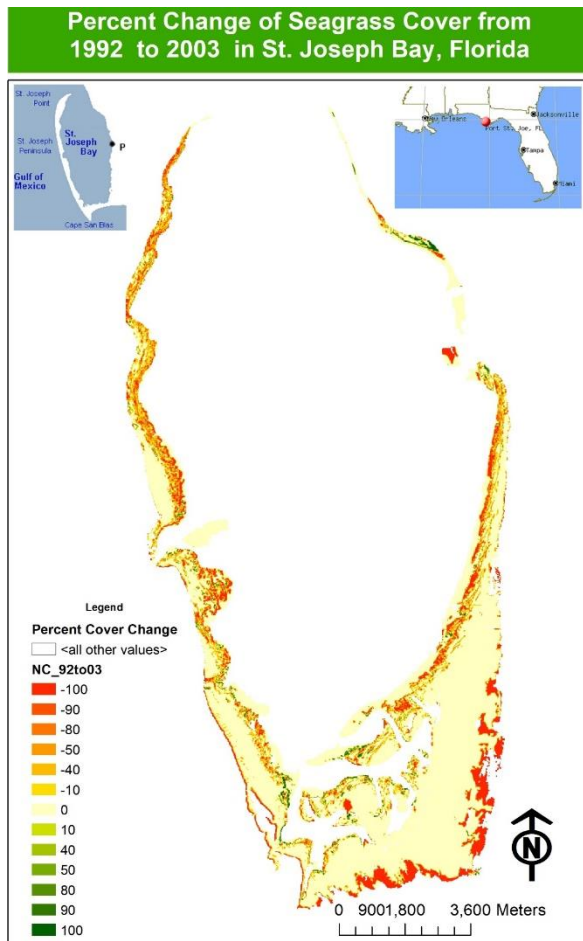


**Figure 13:** map of percent cover change per grid cell from 1959-1980



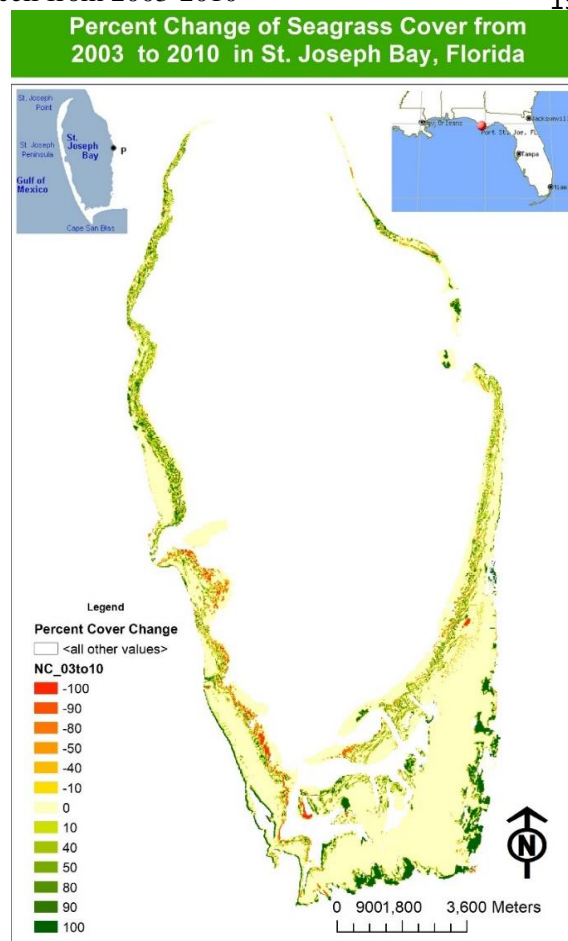
**Figure 14:** map of percent cover change per grid cell from 1980-1992

**Figure 15:** map of percent cover change per grid cell from 1992-2003

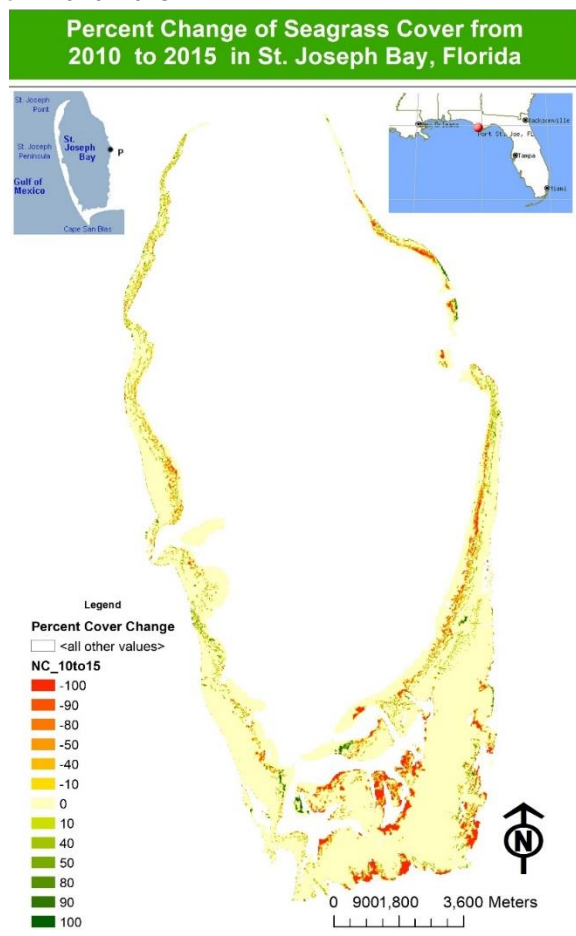


**Figure 16:** map of percent cover change per grid cell from 2003-2010

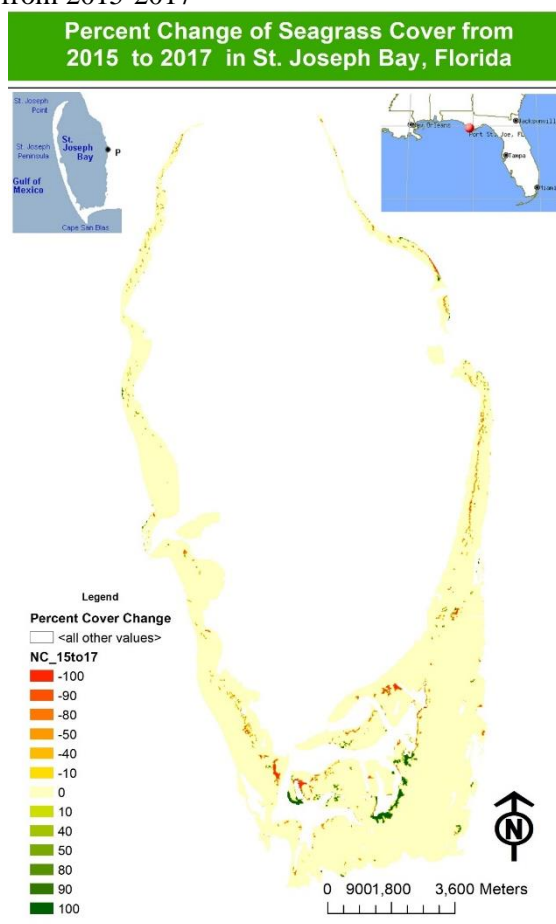
19



**Figure 17:** map of percent cover change per grid cell from 2010-2015



**Figure 18:** map of percent cover change per grid cell from 2015-2017





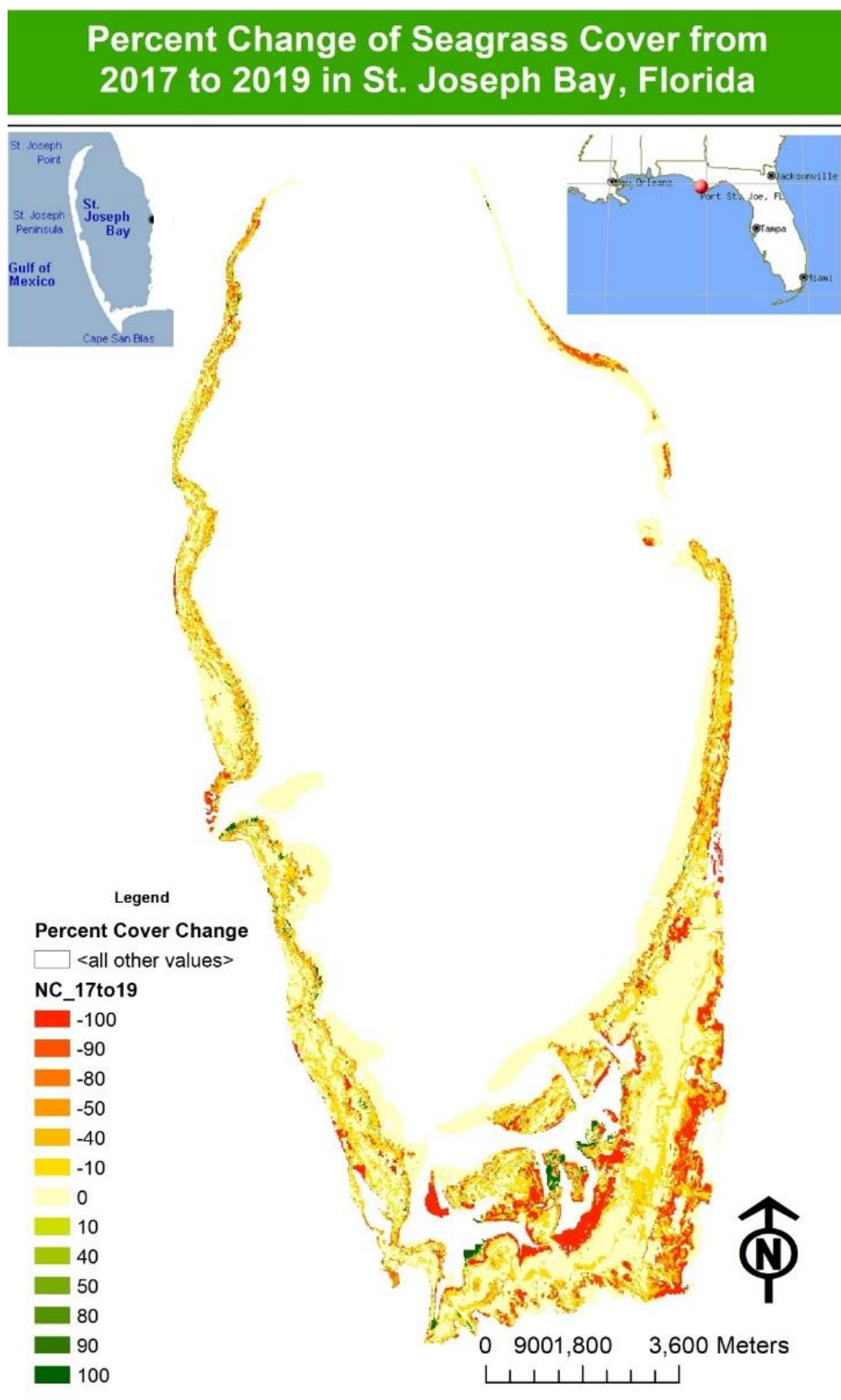


**Figure 19:** Map of percent cover change per grid cell from 2017-2019

From the attribute tables of the previous displayed maps, the following tables and graphs were created. Each classification frequency calculation on the historical cover data as well as the 2019 cover data were grouped together in categories of total cover loss (all grid cells that experienced a negative percent change), gain (all grid cells that experienced a positive percent change), and no change (all grid cells that did not change) since the prior study. The full table of results displaying the frequency, percent of grid, and area (m<sup>2</sup>) for each of the 13 possible percent change per grid cell values, as depicted in figure 10, is found in the appendices.

### Calculated Areas of Total Seagrass Cover Loss, Gain, and No Change

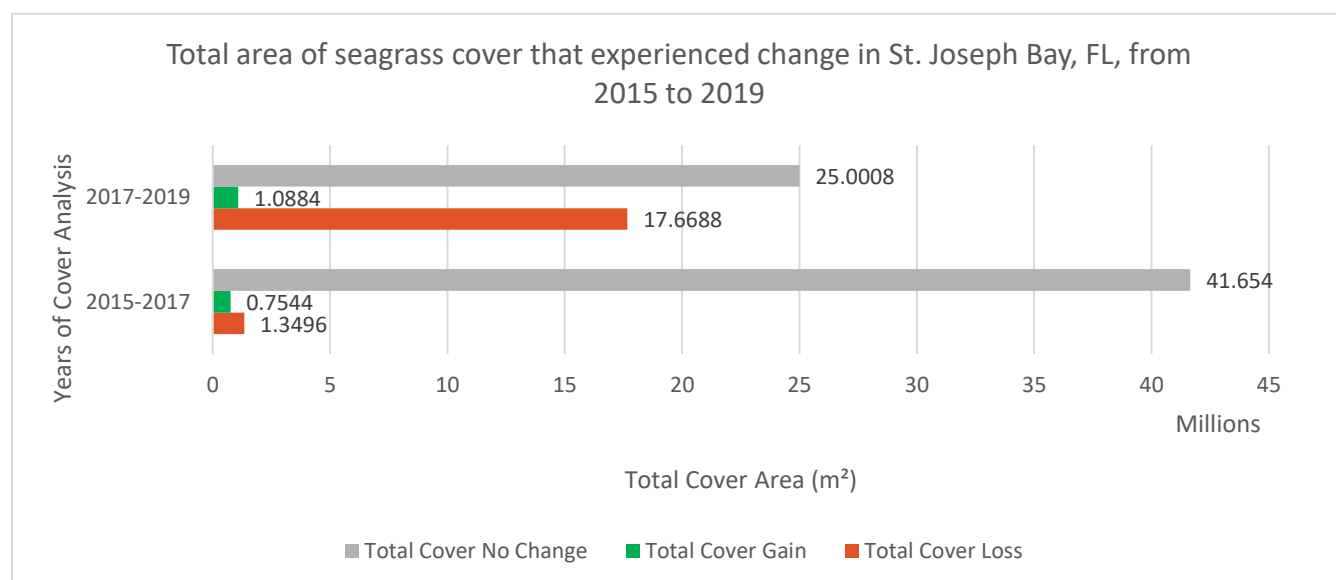
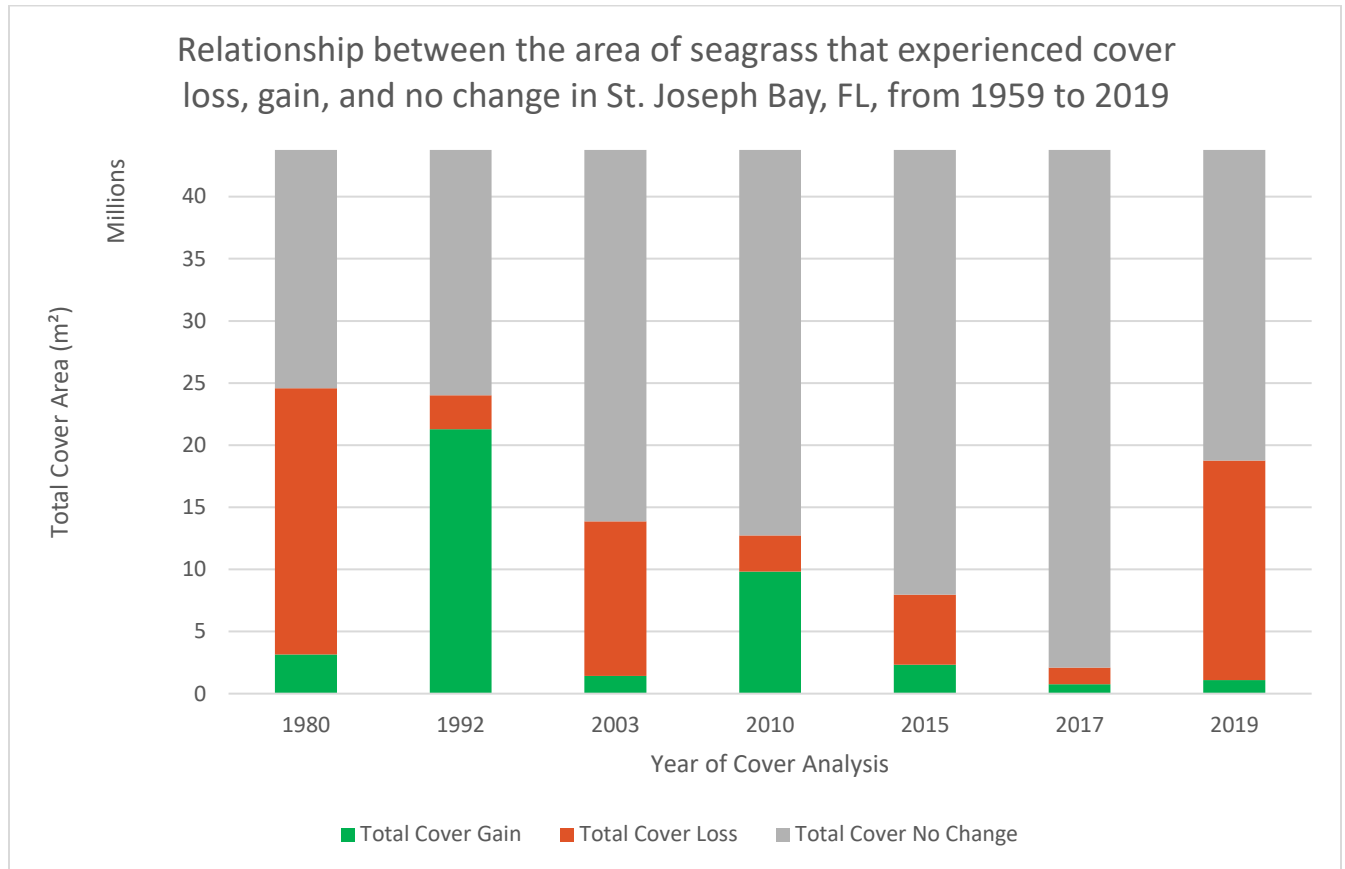


**Figure 20:** Graph comparing the total amount in area of seagrass that experienced any cover gain, loss, and no change between the years 2015-2017 and 2017-2019

	Study 1	Study 2	Study 3	Study 4	Study 5	Study 6	Study 7
	1959-1980	1980-1992	1992-2003	2003-2010	2010-2015	2015-2017	2017-2019
Total Cover Loss (m <sup>2</sup> )	2.14E+07	2.74E+06	1.25E+07	2.89E+06	5.64E+06	1.35E+06	1.77E+07
Total Cover Gain (m <sup>2</sup> )	3.15E+06	2.13E+07	1.42E+06	9.83E+06	2.33E+06	7.54E+05	1.09E+06
Total Cover No Change (m <sup>2</sup> )	1.92E+07	1.97E+07	2.99E+07	3.10E+07	3.58E+07	4.17E+07	2.50E+07

**Figure 21:** Chart displaying the total amount in area of seagrass that experienced any cover gain, loss, and no change between the years 1959-2019

**Figure 22:** Graph comparing the total amount in area of seagrass that experienced any cover gain, loss, and no change between the years 1959-2019



By using an interpretation-based mapping and calculation process, this study found that between 2017 and 2019, St. Joseph Bay approximately 17.6688 km<sup>2</sup> (1766.88 ha) of seagrass cover experienced decline while only 1.0884 km<sup>2</sup> (108.84 ha) experienced cover gain. This recorded cover loss is greater than that of previous cover studies except the study between 1959 and 1980.

#### Calculated Percentage Distribution of Seagrass Cover Loss, Gain, and No Change

	Study 1	Study 2	Study 3	Study 4	Study 5	Study 6	Study 7
	1959-1980	1980-1992	1992-2003	2003-2010	2010-2015	2015-2017	2017-2019
Total Cover Loss (%)	48.97%	6.25%	28.47%	6.61%	12.90%	3.08%	40.38%
Total Cover Gain (%)	7.20%	48.62%	3.24%	22.47%	5.32%	1.72%	2.49%
Total Cover No Change (%)	43.83%	45.12%	68.30%	70.92%	81.79%	95.19%	57.13%

**Figure 23:** Chart displaying percent of St. Joseph Bay seagrass that experienced cumulative cover gain, loss, and no change between the years 1959-2019

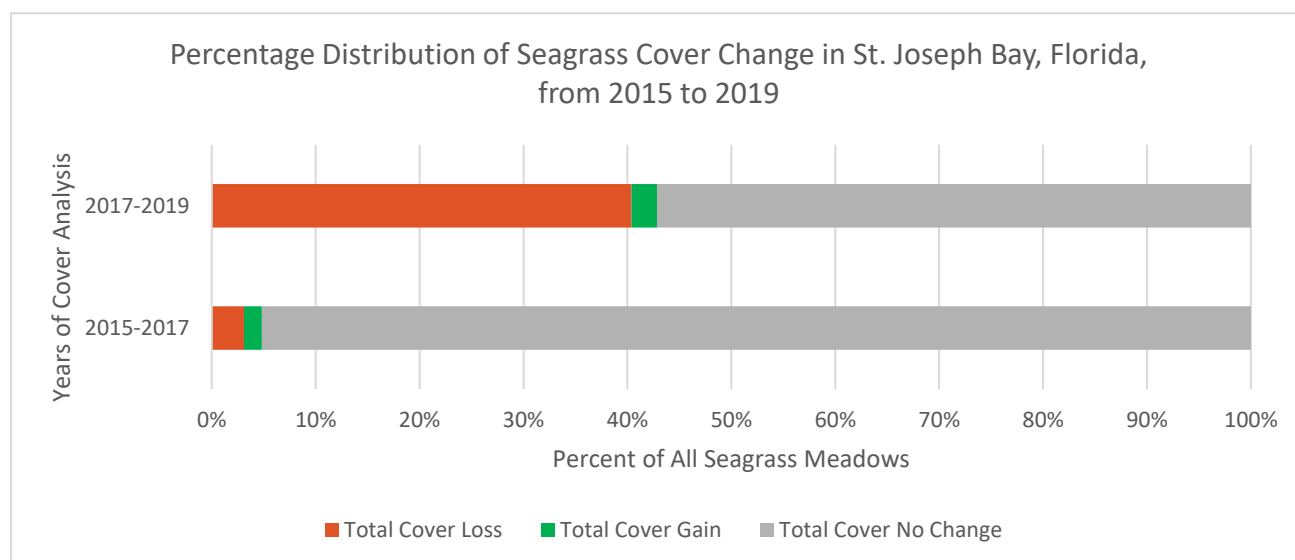


**Figure 24:** Graph comparing percent of St. Joseph Bay seagrass that experienced cumulative cover gain, loss, and no change between the years 2015-2017 and 2017-2019

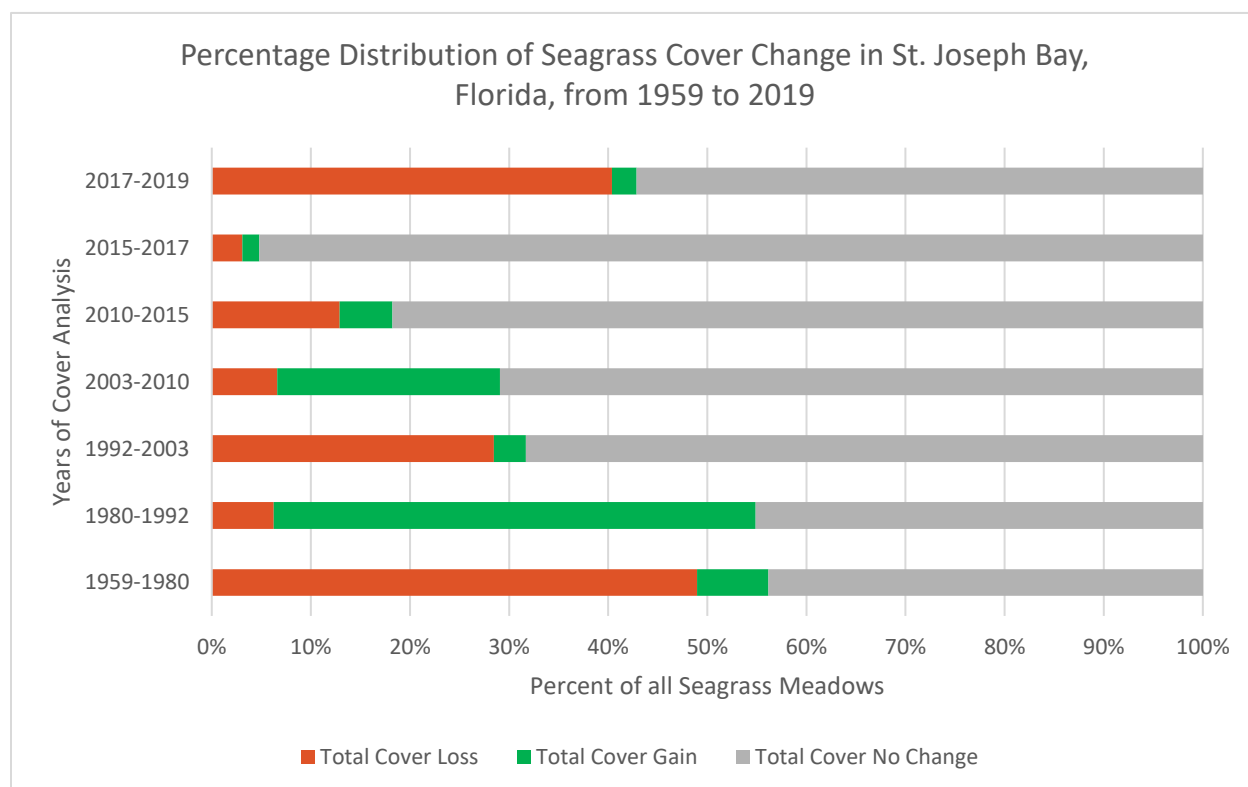


**Figure 25:** Graph comparing percent of St. Joseph Bay seagrass that experienced cumulative cover gain, loss, and no change from 1959-2019

As displayed in figures 11-25, this study found that 40.38% of all seagrass meadows in St. Joseph Bay experienced decline from 2017-2019. 2.49% experienced cover gain while 57.13% did not experience any cover change. Although the spatial extent of cover loss between 2017 and 2019 was less than that of the cover loss between 1959 and 1980, 7.31% of all seagrass meadows experienced a 100% loss in 2017-2019 compared to only 3.93% in 1959-1980.

The study from 1959-1980 is expected to have a net loss, since the study period is 21 years longer than that of the current study and took place during a period of increased human development in Florida. The next study that took place 12 years later (1980-1992), saw that 99% of the loss from decades prior was gained back at the time of the cover analysis in 1992. Considering this, it is possible that the lost cover will recover in the following decades, although the recorded cover gain between 2017 to 2019 was 34.5% less than the cover gain that took place between 1959 and 1980. It must also be noted that the 2.49% cover gain between 2017 and 2019 increased 145% from the 1.72% gain between 2015 and 2017. However, without historical data before 1980, it is impossible to determine any long-term trends.

The provided aerial imagery tiles each had a 10215x10215 pixel resolution for an uncompressed size of 398.05 MB. While interpreting the cover map, this high resolution causes the user's view to change at every data frame scale. This is the scale for the data frame was kept at 1:1250 as a controlled variable. In other words, it is possible to generate different cover maps and accompanying statistics than produced in this study if the imagery were viewed by the user at a larger or smaller scale.

Currently, visual complications are encountered when working with multispectral imagery of littoral zones, caused by factors of water depth, turbidity, atmospheric conditions, surface conditions, currents, epiphytic algae, and sun angle. Similar issues are encountered in

most field experiments, as there are too many variables to control. Such complications could also potentially create a bias in the produced maps of this study. Accuracy of remote automated classification is greatly reduced because of this same problem, which was why the photointerpretation-based classification method was chosen for this study.

## **CONCLUSION**

This study observed that seagrass in St. Joseph Bay experienced a significant decline between 2017 and 2019. Likely, this was caused by combination of multiple stressors present in the area including but not limited to Hurricane Michael, recreational boat propeller scarring, sea urchin grazing, nutrient runoff, water clarity, and phytoplankton. As of 2016, previous FWRI seagrass mapping efforts determined that all but one of these stressors are either episodic or increasing, with propeller scarring determined to be extensive (Yarbro and Carlson 2016). The maps created from this study, using imagery from 2019, indicate continued evidence and extent of this thinning. There is a resulting continued need for restoration and conservation attempts since seagrass beds are so valuable ecologically and economically on both the global as well as local scale. Using the data and statistics generated from the produced maps, areas of highest concern and vulnerability can and will be identified as part of the third “Seagrass Integrated Mapping and Monitoring Program Mapping and Monitoring Report” produced by the Florida Fish and Wildlife Research Institute (FWRI). Seagrass mapping and monitoring is crucial for the effective ecosystem management of St. Joseph Bay.

## WORKS CITED

- Challener, Roberta, et al. "Rapid Assessment of Post-Hurricane Michael Impacts on a Population of the Sea Urchin *Lytechinus Variegatus* in Seagrass Beds of Eagle Harbor, Port Saint Joseph Bay, Florida." *Gulf and Caribbean Research*, vol. 30, 2019, doi:10.18785/gcr.3001.07.
- Eklöf, J.s., et al. "Sea Urchin Overgrazing of Seagrasses: A Review of Current Knowledge on Causes, Consequences, and Management." *Estuarine, Coastal and Shelf Science*, vol. 79, no. 4, 2008, pp. 569–580., doi:10.1016/j.ecss.2008.05.005.
- Iverson, R.L. & H.F. Bittaker, 1986. Seagrass distribution & abundance in the eastern Gulf of Mexico waters. *Estuarine Coast. Shelf Sci.*, Vol. 22, pp. 577-602.
- Erftemeijer, Paul L.A., and Roy R. Robin Lewis. "Environmental Impacts of Dredging on Seagrasses: A Review." *Marine Pollution Bulletin*, Pergamon, 31 Oct. 2006, <https://www.sciencedirect.com/science/article/pii/S0025326X06003778>
- "Florida." NOAA Office for Coastal Management, 10 July 2019, <https://coast.noaa.gov/states/florida.html>.
- Griffiths, Laura L., et al. "Critical Gaps in Seagrass Protection Reveal the Need to Address Multiple Pressures and Cumulative Impacts." *Ocean & Coastal Management*, vol. 183, 1 Jan. 2020, doi:10.1016/j.ocecoaman.2019.104946.
- "Impacts." Impacts, Florida Museum, 3 Oct. 2018, <https://www.floridamuseum.ufl.edu/southflorida/habitats/seagrasses/impacts/>.

Knutson, Thomas, et al. "Tropical Cyclones and Climate Change Assessment: Part II: Projected Response to Anthropogenic Warming." *Bulletin of the American Meteorological Society*, vol. 101, no. 3, 2020, doi:10.1175/bams-d-18-0194.1.

Lamb, Joleah B., et al. "Seagrass Ecosystems Reduce Exposure to Bacterial Pathogens of Humans, Fishes, and Invertebrates." *Science*, vol. 355, no. 6326, 2017, pp. 731–733., doi:10.1126/science.aal1956.

Larkum, A. W. D., et al. *Seagrasses: Biology, Ecology, and Conservation*. Springer, 2011.

Lindsey, Rebecca. "Climate Change: Atmospheric Carbon Dioxide." *Climate.gov*, NOAA, 19 Sept. 2019, <https://www.climate.gov/news-features/understanding-climate/climate-change-atmospheric-carbon-dioxide>.

Matz, Hanover. "Current Threats to Coastal Seagrass Ecosystems." *Shark Research Conservation Program SRC University of Miami*, Rjd  
<https://blog1.Miami.edu/Sharklab/Wp-Content/Uploads/Sites/28/2018/09/Um-Shark-Research-Logo-2018.Jpg>, 18 Mar. 2015, <https://sharkresearch.rsmas.miami.edu/current-threats-to-coastal-seagrass-ecosystems/>.

Nayegandhi, A. Lidar technology overview. *US Geological Survey*, 2007.

Robert J. Orth, Tim J. B. Carruthers, William C. Dennison, Carlos M. Duarte, James W. Fourqurean, Kenneth L. Heck, A. Randall Hughes, Gary A. Kendrick, W. Judson Kenworthy, Suzanne Olyarnik, Frederick T. Short, Michelle Waycott, Susan L. Williams, A Global Crisis for Seagrass Ecosystems, *BioScience*, Volume 56, Issue 12, December 2006, Pages 987–996, [https://doi.org/10.1641/0006-3568\(2006\)56\[987:AGCFSE\]2.0.CO;2](https://doi.org/10.1641/0006-3568(2006)56[987:AGCFSE]2.0.CO;2) Papenbrock, J (2012). "Highlights in seagrass'



phylogeny, physiology, and metabolism: what makes them so species?". International Scholarly Research Network: 1–15

Richard Fox. "Asterias forbesi". Invertebrate Anatomy OnLine. Lander University.

“Seagrass FAQ.” Florida Fish And Wildlife Conservation Commission,

<https://myfwc.com/research/habitat/seagrasses/information/faq/>. El-Hacen, El-Hacen M., et al. “Seagrass Sensitivity to Collapse Along a Hydrodynamic Gradient: Evidence from a Pristine Subtropical Intertidal Ecosystem.” *Ecosystems*, vol. 22, no. 5, 2 Aug. 2019, pp. 1007–1023., doi:10.1007/s10021-018-0319-0.

Sweat, L. H. “Lytechinus Variegatus.” *Indian River Lagoon Species Inventory*, Smithsonian Marine Station at Fort Pierce, 31 Oct. 2012, [naturalhistory2.si.edu/smsfp/irlspec/Lytech\\_varieg.htm](http://naturalhistory2.si.edu/smsfp/irlspec/Lytech_varieg.htm).

Valentine, J F, and K L Heck. “Mussels in Seagrass Meadows: Their Influence on Macroinvertebrate Abundance and Secondary Production in the Northern Gulf of Mexico.” *Marine Ecology Progress Series*, vol. 96, 1993, pp. 215-217., doi:10.3354/meps096063..

Williams, Susan L. “Introduced Species in Seagrass Ecosystems: Status and Concerns.” *Journal of Experimental Marine Biology and Ecology*, vol. 350, no. 1-2, 2007, pp. 89–110., doi:10.1016/j.jembe.2007.05.032.

Wray, Gregory A. "Echinodermata: Spiny-skinned animals: sea urchins, starfish, and their allies". Tree of Life web project, 1999.

Yarbro, L. A., and P. R. Carlson, Jr., eds. 2016. Seagrass Integrated Mapping and Monitoring Program: Mapping and Monitoring Report No. 2. Fish and Wildlife Research Institute Technical Report TR-17 version 2. vi + 281 p.

# APPENDIX 1

1959 to 1980				1980 to 1992				1992 to 2003			
% CC per grid cell	Count	% of grid	Area (m <sup>2</sup> )	% CC per grid cell	Count	% of grid	Area (m <sup>2</sup> )	% CC per grid cell	Count	% of grid	Area (m <sup>2</sup> )
-100	4301	3.932	1720400	-100	13	0.012	5200	-100	8833	8.074	3533200
-90	8984	8.212	3593600	-90	370	0.338	148000	-90	3804	3.477	1521600
-80	1153	1.054	461200	-80	175	0.16	70000	-80	245	0.224	98000
-50	14042	12.836	5616800	-50	1271	1.162	508400	-50	8486	7.757	3394400
-40	2133	1.95	853200	-40	638	0.583	255200	-40	685	0.626	274000
-10	22957	20.985	9182800	-10	4371	3.996	1748400	-10	9088	8.308	3635200
0	47945	43.827	19178000	0	49364	45.125	19745600	0	74712	68.296	29884800
10	3765	3.442	1506000	10	23625	21.596	9450000	10	972	0.889	388800
40	862	0.788	344800	40	1643	1.502	657200	40	475	0.434	190000
50	1862	1.702	744800	50	14853	13.577	5941200	50	1015	0.928	406000
80	206	0.188	82400	80	823	0.752	329200	80	149	0.136	59600
90	809	0.74	323600	90	8773	8.02	3509200	90	584	0.534	233600
100	376	0.344	150400	100	3476	3.177	1390400	100	347	0.317	138800
Total	109395	100	43758000	Total	109395	100	43758000	Total	109395	100	43758000
Total Loss	53570	48.969	21428000	Total Loss	6838	6.251	2735200	Total Loss	31141	28.467	12456400
Total Gain	7880	7.203	3152000	Total Gain	53193	48.625	21277200	Total Gain	3542	3.238	1416800
No Change	47945	43.827	19178000	No Change	49364	45.125	19745600	No Change	74712	68.296	29884800

## APPENDIX 2

2003 to 2010				2010 to 2015				2015 to 2017			
% CC per grid cell	Count	% of grid	Area (m <sup>2</sup> )	% CC per grid cell	Count	% of grid	Area (m <sup>2</sup> )	% CC per grid cell	Count	% of grid	Area (m <sup>2</sup> )
-100	553	0.506	221200	-100	3010	2.751	1204000	-100	352	0.322	140800
-90	868	0.793	347200	-90	1724	1.576	689600	-90	380	0.347	152000
-80	260	0.238	104000	-80	232	0.212	92800	-80	103	0.094	41200
-50	1830	1.673	732000	-50	3495	3.195	1398000	-50	907	0.829	362800
-40	1333	1.219	533200	-40	1434	1.311	573600	-40	481	0.44	192400
-10	2387	2.182	954800	-10	4213	3.851	1685200	-10	1151	1.052	460400
0	77581	70.918	31032400	0	89470	81.786	35788000	0	104135	95.192	41654000
10	7585	6.934	3034000	10	2843	2.599	1137200	10	505	0.462	202000
40	2546	2.327	1018400	40	1472	1.346	588800	40	92	0.084	36800
50	6270	5.732	2508000	50	943	0.862	377200	50	440	0.402	176000
80	615	0.562	246000	80	80	0.073	32000	80	22	0.02	8800
90	2978	2.722	1191200	90	283	0.259	113200	90	219	0.2	87600
100	4589	4.195	1835600	100	196	0.179	78400	100	608	0.556	243200
Total	109395	100	43758000	Total	109395	100	43758000	Total	109395	100	43758000
Total Loss	7231	6.61	2892400	Total Loss	14108	12.896	5643200	Total Loss	3374	3.084	1349600
Total Gain	24583	22.472	9833200	Total Gain	5817	5.317	2326800	Total Gain	1886	1.724	754400
No Change	77581	70.918	31032400	No Change	89470	81.786	35788000	No Change	104135	95.192	41654000

### APPENDIX 3

2017 to 2019			
% CC per grid cell	Count	% of grid	Area (m <sup>2</sup> )
-100	7997	7.31	3198800
-90	4185	3.826	1674000
-80	990	0.905	396000
-50	7258	6.635	2903200
-40	2334	2.134	933600
-10	21408	19.569	8563200
0	62502	57.134	25000800
10	480	0.439	192000
40	714	0.653	285600
50	375	0.343	150000
80	150	0.137	60000
90	454	0.415	181600
100	548	0.501	219200
Total	109395	100	43758000
Total Loss	44172	40.378	17668800
Total Gain	2721	2.487	1088400
No Change	62502	57.134	25000800